Modelling of time dependent plasma plume induced during laser welding

J. Hoffman, T. Mościcki, Z. Szymański

Institute of Fundamental Technological Research
Swietokrzyska 21, 00–049,Warsaw, Poland
e–mail: jhoffman, tmosc, zszym@ippt.gov.pl

Received 28 April 2006

Theoretical modelling of the plasma plume induced during welding of iron sheets with CO_2 laser are presented. The set of equations consists of equation of conservation of mass, energy, momentum and the diffusion equation and is solved with the use of commercially available program Fluent 6.1. The computations are made for the laser power of 1 700 W and shielding gas argon. Two solutions are taken into account stationary and non–stationary. The results show significant difference between these two cases.

PACS: 52.50.Jm, 81.20.Vj
Key words: laser welding, simulations, plasma

1 Introduction

During laser welding, the interaction of intense laser radiation with a workpiece leads to the formation of a long, thin, cylindrical cavity in a metal, called a keyhole. Generation of a keyhole enables the laser beam to penetrate into the workpiece and is essential for deep welding. The keyhole contains ionized metal vapour and is surrounded by molten material called the weld pool. The metal vapour, which flows from the keyhole mixes with the shielding gas flowing from the opposite direction and forms a plasma plume over the keyhole mouth. The plasma plume has considerable influence on the processing conditions. Plasma strongly absorbs laser radiation and significantly changes energy transfer from the laser beam to a material. Although there is comprehensive literature on this topic only few papers treat the problem theoretically [1, 2, 3].

In fact the laser welding process is unstable. The keyhole wall is in permanent non–stationary movement caused by different hydrodynamic instabilities. The variations of the shape of the front wall results in fluctuations of the absorbed laser power and hence in fluctuations of the material evaporation. Similar fluctuations are observed in the radiation of the plasma plume over the keyhole mouth. The characteristic evolution time of the plasma plume is less than 1 ms. It can be then expected that differences between stationary and non–stationary case are serious and the mixing region of both gases, the metal vapour and the shielding gas vary with a time. Unfortunately, the non–stationary model solved in [3] puts emphasis on the first few microseconds of plasma formation and does not consider interaction of the laser beam with the plasma flowing from a keyhole.

In this work time–dependent theoretical modelling of the plasma plume induced during welding of iron with CO_2 laser is presented.

2 Modelling

The set of equations consists of the equation of conservation of mass, energy, momentum and the diffusion equation and is solved in axial symmetry with the use of the commercially available program Fluent 6.1 [4].

$$\frac{\partial \rho}{\partial t} + \nabla \cdot (\rho \mathbf{v}) = 0\,, \tag{1}$$

$$\frac{\partial \rho E}{\partial t} + \nabla \cdot (\mathbf{v}(\rho E + p)) = \nabla \cdot (k \nabla T + \boldsymbol{\phi} \mathbf{v}) + \kappa I_L - R\,, \tag{2}$$

$$\frac{\partial \rho \mathbf{v}}{\partial t} + \nabla \cdot (\rho \mathbf{v}\mathbf{v}) = \nabla p + \nabla \cdot \boldsymbol{\phi} + \rho \mathbf{g} + \mathbf{F}\,, \tag{3}$$

$$\frac{\partial \rho Y_i}{\partial t} + \nabla \cdot (\rho \mathbf{v} Y_i) = \nabla \cdot (\rho D_{i,m} \nabla Y_i)\,, \tag{4}$$

where $\boldsymbol{\phi}$ is the viscous tensor

$$\boldsymbol{\phi} = \mu \left((\nabla \mathbf{v} + \nabla \mathbf{v}^{\mathbf{T}}) - \frac{2}{3} \mathbf{I} \nabla \cdot \mathbf{v} \right)\,. \tag{5}$$

E is energy, $E = h - p/\rho + 0.5v^2$, h enthalpy $h = \sum_j Y_j h_j$, $h_j = \int_{T_{\mathrm{ref}}}^{T} c_{P,j} dT$, ρ is the mass density, p – the pressure, Y_i – the mass fraction of iron vapour in the gas mixture, c_P – specific heat at constant pressure, $\mathbf{v}$ – the velocity vector, k – the thermal conductivity, T – the temperature, κ – the absorption coefficient, I_L – the laser intensity, R – the radiation loss function, $\mathbf{g}$ – the gravity, $\mathbf{F}$ – the external force, μ – the dynamic viscosity, $D_{i,m}$ – the diffusion coefficient, $\mathbf{I}$ – the unit tensor. All the material functions depend on the temperature and mass fraction only.

The source terms including the laser intensity and radiation losses were inserted into the program. It was assumed that the plasma flowing from the keyhole was the ionized iron vapour while the shielding gas was either argon or helium.

The mass densities and the specific heats of argon and iron vapour were calculated assuming the local thermodynamic equilibrium and taking into account the consecutive ionizations stages. The partition functions for argon and iron were taken from [5, 6]. The mixture's density and the mixture's specific heat are computed by the Fluent solver [4].

The viscosity and the thermal conductivity of mixture are computed by the Fluent solver [4] from the formula which are based on kinetic theory and Wilke estimation method [7]. The coefficients of the viscosity and the thermal conductivity of argon were taken from [8]. The viscosity and the thermal conductivity coefficients of iron vapour were taken from [9]. Although the Wilke estimation is not very accurate for plasma it has been found that in our case the values obtained by Fluent are in fair agreement with the values obtained from more rigorous calculations [10]. Similar agreement has been found in the case of thermodynamic properties.

The radiation loss function for the argon-iron mixture was taken from [11]. The radiation loss function calculated in [11] is referred to as the net emission coefficient, which takes into account self–absorption of the radiation. The results depend on the characteristic plasma dimension L, and in our computations we used the results obtained for $L = 1$ mm.

The absorption coefficient of the 10.6 μm was calculated taking into account absorption due to the electron–ion inverse bremsstrahlung and photo–recombination as well as the absorption due to the electron–atom inverse bremsstrahlung. The details of calculation are described in [12].

The mass diffusion coefficient was calculated taking into account relevant collisions between Ar and Fe atoms and ions.

The intensity distribution of CO_2 laser radiation (10.6 μm) was assumed to be Gaussian (TEM_{00} mode). The energy source term was used in the form

$$I_L = \frac{2P_L}{\pi w^2(z)} \exp\left(-\frac{2\,r^2}{w^2(z)} - \int \kappa ds\right), \tag{6}$$

where

$$w^2(z) = w_0^2\left(1 + \left(\frac{z}{z_0}\right)^2\right), \tag{7}$$

and z_0 is the Rayleigh length; r and z are radial and axial coordinate, respectively, κ is the absorption coefficient and the integration is over the distance travelled by the beam. The first part of equation (6) describes focused Gaussian beam and the last exponential component takes into account the attenuation of the laser beam on its way to the point $(r,\ z)$. The mesh grid in the region of the laser beam is fitted to the caustic of the beam so that successive computational cells follow the direction of the laser beam.

The focus spot radius w_0 (within which 86 % of the laser power is contained) was assumed to be equal 0.15 mm and the f-number $= f/D = 7$, where f was the focal length and $D = 2w(f)$ was the diameter of the laser beam at the focusing lens.

The boundary conditions for the above system of equations were as follows. The laser beam and the stream of the shielding gas were directed vertically downwards. The laser power was 1 700 W. The aperture of the shielding gas nozzle was 6 mm in diameter. The inlet velocity of shielding gas was 25 m s^{-1} and the inlet temperature of the shielding argon was 300 K.

The stream of iron vapour was directed vertically upwards from the keyhole mouth 0.4 mm in diameter. The inlet temperature of the iron vapour 10 000 K.

At walls the no–slip boundary and a fixed temperature condition was applied. At the outflow boundary the pressure outlet boundary conditions [4] were used which required the specification of a static pressure at the outlet boundary. This static pressure value is relative to the operating pressure set.

The outflow boundary condition, which assumed a zero normal gradient for all flow variables except pressure was also used but it was found that the use of a pres-

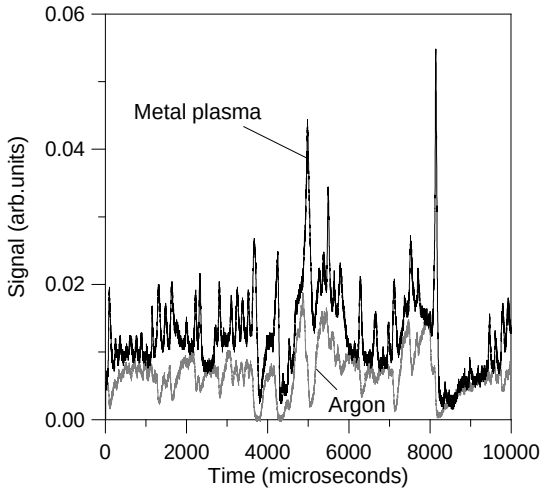

Fig. 1. Signal from photodiode (metal plasma) and monochromator (argon plasma)during welding with CO_2 laser. Laser power is 1 700 W. Material iron sheet 2 mm thick. Welding speed 2 m/min. Argon flow rate 30 litre/min.

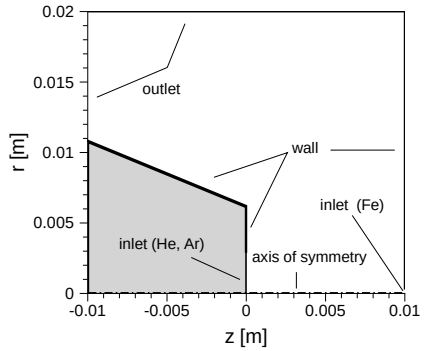

Fig. 2. Calculation domain with boundary conditions.
Nozzle is marked by the shadowed area.

sure outlet boundary condition resulted in better convergence having practically no influence on the results of calculations. The axis boundary conditions were used at the centreline of the axis–symmetric geometry [4].

The Fig. 1 shows the signals from a photodiode (the metal plasma) and from a monochromator set on the Ar I 750.4 nm argon line. The signals show that the plasma appears in pulses with a frequency of $\sim$ 3 kHz. From time to time the plasma extinguishes completely (both signals from metal plasma and argon plasma decrease to zero) and then reappears. Such plasma recovery is considered in this paper.

As the initial condition $t = 0$ it was assumed that the argon flow–field is already stationary at the temperature of 300 K. The laser power is on but the cold argon does not absorb the energy. Then the iron vapour starts flowing from the keyhole mouth. It has been assumed that the metal vapour velocity varies as $v = C\,t^2$, where $C = 4.444 \times 10^9\,\mathrm{m\,s^{-3}}$. After 150 µs, $v = 100\ \mathrm{m\,s^{-1}}$. The value of $100\,\mathrm{m\,s^{-1}}$ was taken from [13].

3 Results

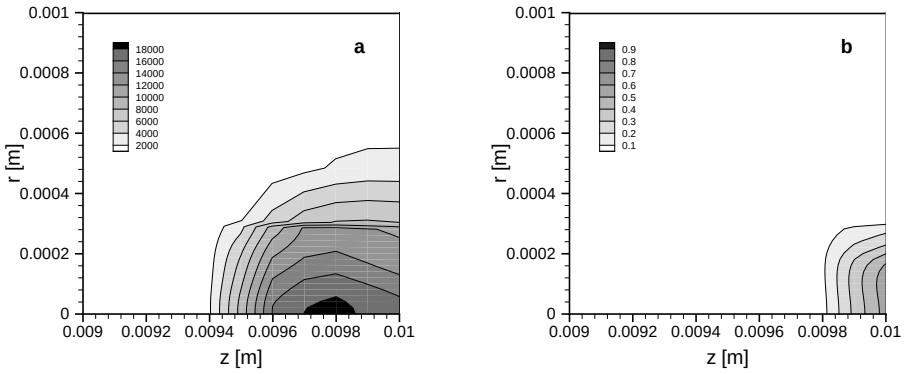

Fig. 3. Temperature distribution (a) and iron mass fraction (b) in plasma induced by laser at $t = 25$ µs. The argon inlet flow is $25\,\mathrm{m\,s^{-1}}$ at 300 K. Iron vapour inlet flow is $100\ \mathrm{m\,s^{-1}}$ at 10 000 K. Laser power is 1 700 W. The outer isotherm is 2 000 K. The isotherms interval is 2 000 K. The metal surface and laser focal plane at $z = 0.01$ m.

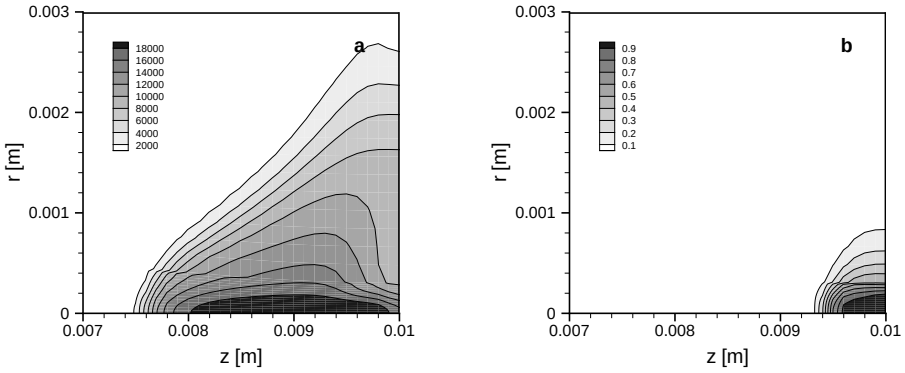

Fig. 4. Temperature distribution (a) and iron mass fraction (b) in plasma induced by laser at $t = 150$ µs. The argon inlet flow is $25\,\mathrm{m\,s^{-1}}$ at 300 K. Iron vapour inlet flow is $100\ \mathrm{m\,s^{-1}}$ at 10 000 K. Laser power is 1 700 W. The outer isotherm is 2 000 K. The isotherms interval is 2 000 K. The metal surface and laser focal plane at $z = 0.01$ m.

The results show that in the case when argon is used as the shielding gas both plasmas the argon and iron plasma are present. The argon plasma starts to develop from the very beginning of the pulse of the hot metal vapour. After 25 μs the metal plasma reaches height of merely 0.2 mm and is diluted by the argon gas (see Fig. 3). The upper half of the plasma situated between $0.0094 < z < 0.0098$ m burns in nearly pure argon and reaches maximum temperature over 18 kK. After 150 μs plasma height reaches 2.5 mm (Fig. 4) and again the argon plasma occupies most of the plume – between $0.0077 < z < 0.0094$ m. The presence of the argon plasma significantly increases absorption of the laser beam which amounts to 40 W and 253 W, i.e. 3.75 % and 15 % of the laser power at 25 and 150 μs, respectively.

4 Conclusion

The non–stationary theoretical model presented above shows that in the case when argon is used as the shielding gas the argon plasma develops very quickly - few microseconds after the metal plasma emerges from a keyhole. Farther both of plasmas the iron plasma and argon plasma exist together. Even after 150 μs the plasma is 40 % smaller than the plasma obtained from the stationary solution [2]. The problem considered in this paper is different than that calculated by Kim and Farson [3] and therefore the comparison of the results is not possible.

This work has been partially supported by Research Project 4TO7A04529.

References

[1] X. Chen, H. Wang: J.Phys D: Appl. Phys. **36** (2003) 1634–1643.

[2] T. Moscicki, J. Hoffman, Z. Szymanski: J. Phys. D: Appl. Phys. **39** (2006) 685–692.

[3] K. R. Kim, D. F. Farson: J. Appl. Phys. **89** (2001) 681–68.

[4] *Fluent 6.1 Users Guide*. Fluent Inc., Lebanon NH 2005.

[5] H. W. Drawin, P. Felenbock: *Data for plasmas in local thermodynamic equilibrium*. Gauthier–Villars, Paris 1965.

[6] J. Halenka, B. Grabowski: Astron. Astrophys. Suppl. Ser. **57** (1984) 43–49.

[7] R. C. Reid, T. K. Sherwood: *The properties of gases and liquids*. McGraw–Hill Book Company, New York 1966.

[8] R. S. Devoto: The Physics of Fluids **165** (1973) 616–623.

[9] K. Makowski: J. Tech. Physics **39** (1998) 37–66.

[10] T. Amakawa, K. Adachi, Y. Ohki, T. Inaba: Trans. IEE Japan **119–A** (1999) 75–79.

[11] J. Menart, S. Malik: J. Phys. D: Appl. Phys. **35** (2002) 867–874.

[12] J. Hoffman, Z. Szymaski: Opt. Applicata **32** (2002) 129–145.

[13] E. Beyer: *Schweissen mit laser*. Springer–Verlag, Berlin 1995.